# DYNAMICS OF MELITTIN IN WATER AND MEMBRANES AS DETERMINED BY FLUORESCENCE ANISOTROPY DECAY

EDGAR JOHN AND FRITZ JÄHNIG
*Max-Planck-Institut für Biologie, Corrensstr. 38, 7400 Tübingen, Federal Republic of Germany*

ABSTRACT  Fluorescence anisotropy decay measurements were performed on melittin in water and in membranes of dimyristoylphosphatidylcholine. The fluorescence of the single tryptophan residue of melittin and of a pyrene label attached to melittin was detected. In water, the slowest relaxation process in the anisotropy decay occurs with a relaxation time of 1.5 or 5.5 ns in the case of low or high ionic strength and corresponds to rotational diffusion of monomeric or tetrameric melittin. Superimposed on this slow process are fast processes in the subnanosecond range reflecting fluctuations of the fluorophores relative to the polypeptide backbone. In membranes, the fast relaxation processes are not much altered. A slow process with a relaxation time of 35 ns is observed and assigned to orientational fluctuations of the melittin helices in membranes.

## INTRODUCTION

The polypeptide melittin, consisting of 26 residues, is often studied as a simple model for membrane proteins. It has been shown to function as a voltage-gated pore (Tosteson and Tosteson, 1981; Tosteson et al., 1987; Kempf et al., 1982; Hanke et al., 1983). Melittin differs, however, from a genuine membrane protein by its much more complex phase diagram. For example, melittin is soluble in water and even exists in two forms in water. At low concentration and low ionic strength, it is monomeric with a random conformation, while at high concentration and/or high ionic strength it adopts a largely helical conformation and aggregates as a tetramer (Talbot et al., 1979; Quay and Condie, 1983). The x-ray structure of the water-soluble tetramer has been determined (Terwilliger et al., 1982). There is increasing evidence that in membranes of lipid vesicles melittin also can exist in two forms, a monomeric and an oligomeric one. Vogel and Jähnig (1986) have shown that this equilibrium depends on the melittin concentration and presented evidence for a tetrameric aggregation, while Talbot et al. (1987) found that, in addition, the equilibrium depends on ionic strength. A further transition in the phase diagram of melittin occurs when the melittin/lipid mole ratio exceeds 1:30. Then the vesicles undergo a transition to discs (Dufourc et al., 1986). Much of the confusion about the structure of melittin in membranes seems to arise from this complex phase diagram.

Not much is known about the structure of monomeric melittin in membranes, simply because the spectroscopic measurements on membrane-bound melittin have been performed at relatively high concentrations. Typical melittin/lipid mole ratios are 1:100 so that the measurements refer to oligomeric melittin. The conformation of melittin in the oligomer is predominantly α-helical (Lavialle et al., 1982; Vogel and Jähnig, 1986). On the average, the α-helices are oriented parallel to the membrane normal (Vogel et al., 1983; Vogel, 1987). Based on these and other data, Vogel and Jähnig (1986) proposed a model for the aggregated form of melittin in membranes in which four membrane-spanning helices form a bundle with their hydrophilic sides facing each other and their hydrophobic sides facing the lipids. This tetramer could act as a membrane pore. Since then, experimental results have been reported which lend further support to the model (Vogel, 1987; Talbot et al., 1987), while others are at variance with it (Hermetter and Lakowicz, 1986; Stanislawski and Rüterjans, 1987).

Besides the structure, the dynamics of melittin may well play a role in its functioning as a membrane pore. Within the above model, it would be of special interest to know whether the membrane-spanning helices maintain a fixed orientation or undergo orientational fluctuations in fulfillment of the pore function. This question was one reason for us to perform fluorescence anisotropy decay (FAD) measurements on melittin in membranes. The other reason was that large transport proteins often consist of a number of membrane-spanning helices, and orientational fluctuations of these helices were shown to be necessary for transport (Dornmair, K., and F. Jähnig, manuscript submitted for publication). Here, melittin may serve as a simple model to study orientational fluctuations of helices in membranes. Orientational fluctuations of lipid molecules have relaxation times of about a nanosecond (Best et al., 1987). One would then expect the orientational fluctuations of membrane-spanning helices to be slower and relax with typical times in the range of tens of nanoseconds.

Melittin has one Trp residue at position 19 which can be used as an intrinsic fluorophore in FAD measurements. In the model of Vogel and Jähnig (1986), Trp 19 is located at the end of but still on the membrane-spanning helices. Fluctuations of Trp residues in soluble proteins have been detected by the FAD technique (for a review see Beecham and Brand, 1985). Typical relaxation times range from below a nanosecond to several nanoseconds and the underlying relaxation processes have been assigned to fluctuations of the Trp side chain relative to the polypeptide backbone and to fluctuations of the backbone up to rotational diffusion of the entire protein. Fluctuations of the backbone may occur, for example, as bending oscillations of a helix or as orientational fluctuations of the helix. Bending oscillations are fast with typical times of a few picoseconds (Pleiss, J., and F. Jähnig, manuscript in preparation), whereas orientational fluctuations are expected to be slow with times in the range of tens of nanoseconds, similar to the case of a membrane-spanning helix. In both cases, such slow fluctuations would be difficult to detect via the fluorescence of Trp residues, because of the short lifetime of only 3 ns of the Trp fluorescence. This problem may be solved in two ways: either by detecting the Trp anisotropy much more accurately than usual with prolonged sampling of data, or by using a fluorophore with a longer lifetime.

FAD measurements on water-dissolved melittin have been performed with detection of the fluorescence of Trp (Georghiou et al., 1982; Tran and Beddard, 1985; Lakowicz et al., 1986) or of an anthraniloyl label (Maliwal et al., 1986). Several relaxation processes were observed, the fast ones corresponding to fluctuations of the fluorophores relative to the backbone and the slowest one corresponding to rotational diffusion. However, the values obtained for the relaxation time of rotational diffusion of the monomer range from 1 to 10 ns and for the tetramer from 2 to 14 ns.

FAD measurements on the Trp fluorescence of membrane-incorporated melittin have also been reported. In one case, the data were analyzed in terms of one relaxation time and a value of 10 ns was obtained which is difficult to assign to any fluctuation (Georghiou et al., 1982). In the other case, three relaxation times were found, the largest one being 20 ns (Vogel and Rigler, 1987). This slow relaxation process was assigned to fluctuations of membrane-spanning helices formed by melittin. As discussed above, determination of such a long relaxation time via Trp fluorescence is unreliable under the usual experimental conditions and, therefore, the result of Vogel and Rigler must be considered with caution. Maliwal et al. (1986) using an anthraniloyl label with a longer lifetime detected again two fast processes and a slow one, the latter having a relaxation time of 50 ns. The data analysis, however, was performed under the assumption of an isotropic environment of the label which is not justified in the case of membrane-incorporated melittin. Therefore, this result

also is not reliable. In summary, FAD data on the dynamics of melittin are available, but they either differ among each other or are unreliable. In this situation, we decided to make another effort to determine the relaxation times of rotational diffusion of melittin in water and especially of the helix fluctuations of melittin in membranes. In the latter case, we followed the two strategies mentioned above to determine a relaxation time in the range of tens of nanoseconds. The Trp fluorescence was sampled over much longer times than usual, and pyrene-maleimide was attached to melittin serving as a fluorophore with a long lifetime component. Agreement between the values obtained with the two approaches for the slow relaxation time was considered as a strong test for the reliability of the result.

## MATERIALS AND METHODS

### Chemicals

Dimyristoylphosphatidylcholine (DMPC) was purchased from Fluka and used without further purification. Pyrene-maleimide (MalNPyr) was obtained from Serva Fine Biochemicals Inc., Garden City Park, NY. 2,5-bis(4-Biphenylyl)-oxazole (BBO) and 1,6-diphenyl-1,3,5-hexatriene (DPH) were from EGA-Chemie, Steinheim, FRG, p-terphenyl (PTP) was from Sigma Chemical Co., St. Louis, MO, and phenanthrene from Serva Fine Biochemicals Inc. All solvents were from E. Merck, Darmstadt, FRG, and were of spectroscopic grade.

### Purification and Labeling of Melittin

Melittin was purchased from Serva Fine Biochemicals Inc. and purified according to the procedure of B. Wille (manuscript in preparation). After the purification, phospholipase activity could no longer be detected. Melittin labeled with MalNPyr was a gift of B. Wille from this institute. Labeling had been performed as described by Wille, B., H. Kiefer, E. John and F. Jähnig (manuscript in preparation). Melittin labeled that way with pyrene is still water soluble and acts as a voltage-gated pore like unmodified melittin (Wille et al., manuscript in preparation).

### Sample Preparation

To prepare vesicles of lipid and melittin, DMPC was dissolved in chloroform and the solvent evaporated under a stream of nitrogen. Buffer (10 mM potassium hydrogen phosphate, pH 7.4) was added to obtain a lipid concentration of 12 mM, then the sample was sonicated in a bath-sonicator for 30 min followed by incubation for 2 h at 36°C. Melittin in the same buffer was added to yield a final lipid concentration of 3 mM and a lipid/melittin mole ratio of 150.

To prepare a film of lipid and melittin on a quartz glass slide, 0.5 mg melittin was mixed equimolar with DMPC in 20 μl methanol. The mixture was deposited on the glass slide and dried under a stream of nitrogen. A transparent film was obtained extended over a region of ~5 mm in diameter. For background measurement, a region of the glass slide outside the film was irradiated.

To prepare vesicles of lipid and MalNPyr-labeled melittin, DMPC and an appropriate amount of MalNPyr-melittin were mixed in methanol. After rotary-evaporation of the solvent, buffer was added and the sample sonicated and incubated as described above. The final concentration of lipid was 1.5 mM and the lipid/MalNPyr-melittin mole ratio 200.

To prepare vesicles of lipid and the MalNPyr label alone, PyrM was first reacted with mercaptoethanol in ethanolic solution yielding 2-ethanol-3'-(N-1''-pyrenyl)succinimidyl-sulfide (MalNPyr-MEt). An appropriate amount of the stock solution was added to preformed DMPC

vesicles at 1.5 mM concentration in buffer. The volume of the added stock solution was below 1% and the lipid/MalNPyr-MEt mole ratio was 200.

To each vesicle sample, a control sample was prepared without the fluorophore.

Before starting a series of measurements, the samples were cooled below the lipid phase transition temperature at 24°C and warmed up to 36°C again to avoid any hysteresis effect of the phase transition. After finishing the measurements, the size and shape of the vesicles was controlled by electron microscopy. Almost all vesicles were unilamellar with diameters between 50 and 200 nm.

The samples used as fluorescence standards were a 5 $\mu$M solution of PTP or a 1 $\mu$M solution of BBO in cyclohexane. The control sample in both cases was cyclohexane. The samples used as anisotropy standards were a 160 $\mu$M solution of phenanthrene or a 5 $\mu$M solution of DPH in cyclohexane.

## FAD Measurements

The apparatus used for the FAD measurements has been described previously (Best et al., 1987). A mode-locked argon-ion laser synchronously pumps a cavity-dumped dye laser to generate light pulses at a repetition rate of 4 MHz. To excite Trp fluorescence, we used rhodamine 6G as laser dye and set the wavelength of the exciting light, after frequency doubling, at $\lambda_{ex} = 300$ nm. To excite MalNPyr fluorescence, rhodamine 101 was used and $\lambda_{ex} = 333$ nm. The emission wavelength was selected by a monochromator, slit width 6 nm, in combination with a cutoff filter (Schott WG 345/4) and was set at $\lambda_{em} = 360$ nm for the Trp fluorescence and at $\lambda_{em} = 395$ nm for MalNPyr fluorescence.

The sample holder could be rotated to bring four different 1 × 1 cm quartz cuvettes into the exciting beam. They contain the sample, the control sample, the fluorescence standard sample, and the control sample for the fluorescence standard. The cuvettes are thermostated and stirred magnetically.

To investigate a lipid/melittin film on a quartz slide, the sample holder was replaced by a XYZ manipulator with the slide mounted on it. The slide was oriented under 45° to the exciting beam and with the film on the backside. In this geometry, the reflected light has a direction opposite to the detection system.

## Data Analysis

The data were analyzed according to the procedure described by Best et al. (1987). The measured intensities of the samples are corrected for background by subtracting the intensities of the control samples. The intensities thus obtained are deconvoluted using a fluorescence standard. This yields the intensities $I_{\parallel}(t)$ and $I_{\perp}(t)$ of the fluorescence light polarized parallel and perpendicular to the exciting light. The total fluorescence or sum is obtained as $S = I_{\parallel} + 2\beta I_{\perp}$, the difference as $D = I_{\parallel} - \beta I_{\perp}$, and the anisotropy as $R = D/S$. $\beta$ is a correction factor accounting for different efficiencies of the detection system for parallel and perpendicular polarized light. The sum $S(t)$ and the difference $D(t)$ were fitted by analytical expressions for the sum

$$s(t) = \sum_{i=1}^{N} a_i e^{-t J_i}, \tag{1}$$

($J_i$ increasing with $i$) and for the anisotropy

$$r(t) = \sum_{i=1}^{M} b_i e^{-t \phi_i} + r_{\infty}, \tag{2}$$

so that $d(t) = r(t) \cdot s(t)$. The partial amplitudes $\alpha_i$ of the sum, the average lifetime $\bar{\tau}$, the initial anisotropy $r_0$, and the average relaxation time $\bar{\phi}$ are obtained as

$$\alpha_i = a_i \Big/ \sum_{j=1}^{N} a_j \tag{3}$$

$$\bar{\tau} = \sum_{i=1}^{N} \alpha_i \tau_i \tag{4}$$

$$r_0 = \sum_{i=1}^{M} b_i + r_{\infty} \tag{5}$$

$$\bar{\phi} = \sum_{i=1}^{M} b_i \phi_i \Big/ \sum_{i=1}^{M} b_i. \tag{6}$$

The assumption of an exponential decay of the anisotropy as in Eq. 2 is reasonable for the case of only one fluorescence transition, i.e., one absorption and one emission dipole. In this case, explicit expressions for $r_0$ and $r_{\infty}$ are available (Szabo, 1980; Zannoni, 1981; van der Meer et al., 1984).

$$r_0 = \tfrac{2}{5} P_2(\theta_a - \theta_e) \tag{7}$$

$$r_{\infty} = \tfrac{2}{5} P_2(\theta_a) \, P_2(\theta_e) \, \langle P_2 \rangle^2, \tag{8}$$

Here, $\theta_a$ and $\theta_e$ are the angles of the absorption and emission dipoles relative to the symmetry axis of the fluorophore assumed to be a symmetric ellipsoid, $P_2(\theta) = (3 \cos^2 \theta - 1)/2$ denotes the second order Legendre polynomial, and $\langle P_2 \rangle$ the orientational order parameter of the fluorophore. The latter is the average of $P_2(\vartheta)$ over the angles $\vartheta$ specifying the instantaneous orientations of the fluorophore relative to its mean orientation. The order parameter of a fluorophore in general results from a superposition of different fluctuations with individual order parameters $\langle P_2 \rangle_i$ so that $\langle P_2 \rangle = \Pi_{i=1}^{M} \langle P_2 \rangle_i$ (Jähnig, 1979). The individual order parameters may be derived from the amplitudes $b_i$ of the individual relaxation processes. The order parameter of the slowest relaxation process, e.g., follows from the relation

$$r_{\infty} = (b_M + r_{\infty}) \langle P_2 \rangle_M^2. \tag{9}$$

Here we have assumed in addition that one of the two angles $\theta_a$ or $\theta_e$ is zero. The total order parameter can be obtained from the relation

$$r_{\infty} = r_0 \langle P_2 \rangle^2. \tag{10}$$

If the fluorophore has more than one transition, the above relations require some modification. For simplicity, we consider the case of two transitions under the following assumptions. (a) The two transitions have different lifetimes $\tau_1$ and $\tau_2$ with relative amplitudes $\alpha_1$ and $\alpha_2 = 1 - \alpha_1$. (b) The two absorption dipoles coincide and are oriented along the symmetry axis of the fluorophore, $\theta_{a1} = \theta_{a2} = 0$, whereas the emission dipoles differ, $\theta_{e1} \neq \theta_{e2}$. Then one obtains

$$r_0 = \tfrac{2}{5} [\alpha_1 P_2(\theta_{e1}) + \alpha_2 P_2(\theta_{e2})] \tag{11}$$

$$r_{\infty}(t) = \tfrac{2}{5} [\alpha_1 e^{-t/\tau_1} P_2(\theta_{e1}) + \alpha_2 e^{-t} J_2 P_2(\theta_{e2})] s^{-1}(t) \langle P_2 \rangle^2 \tag{12}$$

with

$$s(t) = \alpha_1 e^{-t/\tau_1} + \alpha_2 e^{-t} J_2.$$

$r_{\infty}$ is no longer a constant but varies in time as the contributions of the two transitions to the intensity vary. It is still defined as the value of $r(t)$ for $t \gg \phi_i$. Only at times $t \gg \tau_1$ with $\tau_1 \ll \tau_2$ one obtains

$$r_{\infty} = \tfrac{2}{5} P_2(\theta_{e2}) \langle P_2 \rangle^2. \tag{13}$$

The time-dependent anisotropy now becomes

$$r(t) = [\alpha_1 e^{-t/\tau_1} P_2(\theta_{e1}) + \alpha_2 e^{-t/\tau_2} P_2(\theta_{e2})] s^{-1}(t) \left[ \sum_{i=1}^{M} \beta_i e^{-t/\phi_i} + \beta_{M+1} \right]. \tag{14}$$

with $\beta_{M+1} = \frac{2}{5} \langle P_2 \rangle^2$. The coefficients $\beta_i$ are normalized such that $\Sigma_{i-1}^{M+1}$ $\beta_i = \frac{2}{5}$.

The goodness of the fits was examined by visual inspection of the residuals and by comparison of the corresponding $\chi^2$ values. The error limits given in the tables are calculated as standard deviations obtained from the derivatives of $\chi^2$ with respect to the corresponding parameter. They refer to measurements on one sample; the error arising from measurements on different samples is usually larger.

The residuals obtained show pronounced oscillations with a period of 3 ns. Such oscillations have already been observed by others (Turko et al., 1983) and have been traced back to a nonlinear behavior of the time-to-amplitude converter at high counting rates. We confirmed this in control experiments.

## Fluorescence and Anisotropy Standards

Use of a fluorescence standard for deconvolution requires an exact value of its lifetime. This has to be determined once by deconvolution with the apparatus response function. We obtained the response function by light scattering from cyclohexane at the excitation wavelength used for the fluorescence measurement with the analyzer set at the magic angle of 54.7°. In the deconvolution of fluorescence standard data with the response function allowance must be made for a time shift between the two data sets which arises from the different wavelengths of detection (Lambert et al., 1983). We used two fluorescence standards: PTP for Trp fluorescene and BBO for MalNPyr fluorescence. For the lifetimes of PTP and BBO we obtained 0.97 ± 0.01 ns and 1.00 ± 0.01 ns, respectively. The literature values are 0.99 ns for PTP (Wijnaendts van Resandt et al., 1982) and 1.15 ns for BBO (Berlman, 1971).

To determine the correction factor $\beta$ accounting for different efficiencies of the detection system for parallel and perpendicular polarized light we employed a fluorophore with a long lifetime $\tau$ and a short relaxation time $\phi$ of the anisotropy in an isotropic medium. Then the anisotropy at $t \gg \phi$ is zero, while the intensities $I_\parallel$ and $I_\perp$ can still be detected with sufficient accuracy. From the condition $I_\parallel = \beta I_\perp$ the factor $\beta$ is obtained. As anisotropy standards we used phenanthrene at $\lambda_{em} = 360$ nm for

analysis of Trp fluorescence yielding $\beta = 1.06$, and DPH at $\lambda_{em} = 395$ nm for MalNPyr yielding $\beta = 1.17$.

## RESULTS

### Melittin in Water

Fig. 1 shows the intensity and anisotropy of the Trp fluorescence of melittin in water at a concentration of $10^{-5}$ M, pH 7.4, for low and high ionic strength. Under these conditions, melittin is monomeric or tetrameric, respectively (Talbot et al., 1979; Quay and Condie, 1983). The fluorescence decay is slightly faster for the tetrameric state, whereas the anisotropy decays slower. The results of the fits of the intensity and anisotropy by sums of exponentials are listed in Table I. The parameters obtained with two lifetimes are in rough agreement with the results of Georghiou et al. (1982) and Tran and Beddard (1985). The goodness of the fit, however, increased upon inclusion of a third lifetime, whereas a fourth component did not lead to any improvement (the two longest lifetimes simply became identical). This has already been found by Lakowicz et al. (1986), and their values for the three lifetimes and amplitudes are in good agreement with ours.

The anisotropy decay for both monomeric and tetrameric melittin was also fitted first by two exponentials. One relaxation time was found in the subnanosecond range, the other was 1.5 ns for the monomer and 4.9 ns for the tetramer. Upon inclusion of a third relaxation time, nothing changes for the monomer (the longer relaxation time was found twice), but for the tetramer the fit became better as indicated by the $\chi^2$ values. The short relaxation
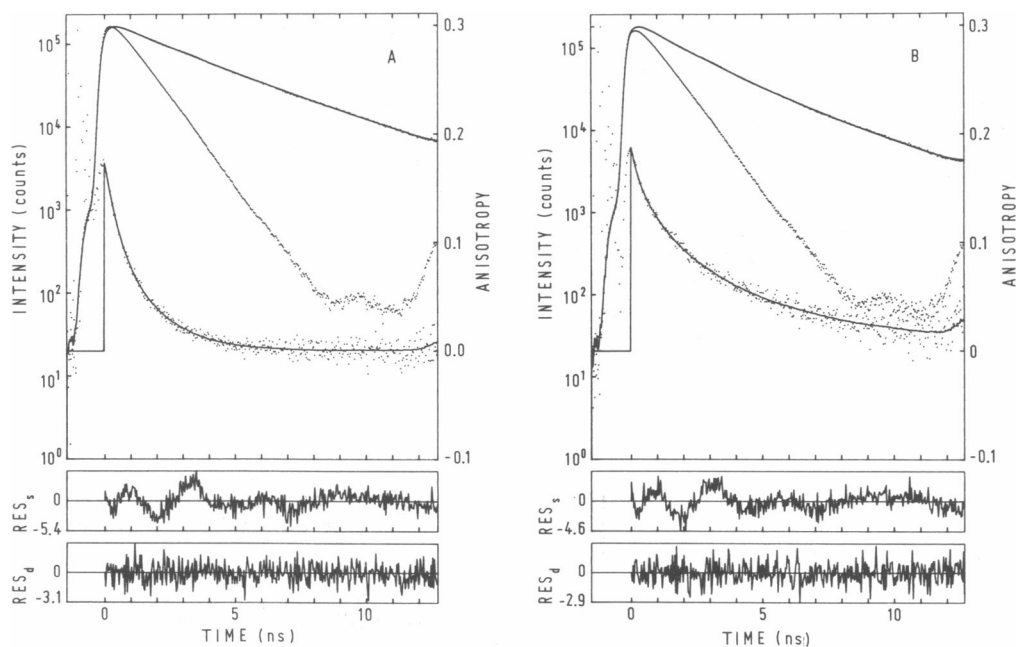


FIGURE 1 Intensity and anisotropy of the Trp fluorescence of melittin in buffer (10 mM potassium phosphate, pH 7.4) at 20°C and 0 M (A) or 2 M NaCl (B). The melittin concentration was 10 $\mu$M (A) or 15 $\mu$M (B). The experimental data (including the fluorescence standard) are shown (. . . .) together with the fits (——) and the corresponding residuals (lower parts). The intensity was fitted by three exponentials and the anisotropy by two exponentials (A) or three exponentials (B).

| | 0 M NaCl | | 2 M NaCl | |
|---|---|---|---|---|
| $\tau_1$ (ns), $\alpha_1$ | 1.29 ± 0.01 | 0.295 ± 0.002 | 1.55 ± 0.01 | 0.598 ± 0.003 |
| $\tau_2$ (ns), $\alpha_2$ | 3.91 ± 0.01 | 0.705 ± 0.003 | 3.78 ± 0.01 | 0.402 ± 0.004 |
| $\bar{\tau}$ (ns) | 3.1 | | 2.4 | |
| $\chi^2$ | 4.11 | | 3.65 | |
| $\tau_1$ (ns), $\alpha_1$ | 0.53 ± 0.03 | 0.17 ± 0.01 | 0.50 ± 0.03 | 0.18 ± 0.01 |
| $\tau_2$ (ns), $\alpha_2$ | 2.6 ± 0.2 | 0.50 ± 0.04 | 2.03 ± 0.04 | 0.61 ± 0.01 |
| $\tau_3$ (ns), $\alpha_3$ | 4.7 ± 0.2 | 0.34 ± 0.05 | 4.5 ± 0.1 | 0.21 ± 0.02 |
| $\bar{\tau}$ (ns) | 3.0 | | 2.3 | |
| $\chi^2$ | 2.80 | | 2.12 | |
| $\tau_1$ (ns), $\alpha_1$ | | | 0.50 ± 0.03 | 0.18 ± 0.01 |
| $\tau_2$ (ns), $\alpha_2$ | | | 2.03 ± 0.04 | 0.61 ± 0.01 |
| $\tau_3$ (ns), $\alpha_3$ | | | 4.50 ± 0.90 | 0.11 ± 0.15 |
| $\tau_4$ (ns), $\alpha_4$ | | | 4.52 ± 0.90 | 0.10 ± 0.15 |
| $\bar{\tau}$ (ns) | | | 2.3 | |
| $\chi^2$ | | | 2.13 | |
| $\phi_1$ (ns), $b_1$ | 0.33 ± 0.03 | 0.084 ± 0.014 | 0.46 ± 0.02 | 0.075 ± 0.005 |
| $\phi_2$ (ns), $b_2$ | 1.54 ± 0.04 | 0.128 ± 0.003 | 4.88 ± 0.07 | 0.136 ± 0.002 |
| $r_\infty$ | | 0.0 (fixed) | | 0.0 (fixed) |
| $r_0$ | | 0.212 | | 0.211 |
| $\bar{\phi}$ (ns) | 1.1 | | 3.3 | |
| $\chi^2$ | 1.02 | | 1.11 | |
| $\phi_1$ (ns), $b_1$ | 0.33 ± 4.0 | 0.084 ± 0.08 | 0.16 ± 0.08 | 0.07 ± 0.07 |
| $\phi_2$ (ns), $b_2$ | 1.53 ± 1.5 | 0.058 ± 0.35 | 1.15 ± 0.09 | 0.054 ± 0.006 |
| $\phi_3$ (ns), $b_3$ | 1.54 ± 1.5 | 0.070 ± 0.07 | 5.56 ± 0.33 | 0.117 ± 0.003 |
| $r_\infty$ | | 0.0 (fixed) | | 0.0 (fixed) |
| $r_0$ | | 0.212 | | 0.239 |
| $\bar{\phi}$ (ns) | 1.1 | | 3.0 | |
| $\chi^2$ | 1.02 | | 1.03 | |

*As shown in Fig. 1.

time split off into two, and the longer one increased to 5.5 ns. This is exactly the value obtained by Lakowicz et al. (1986) from a fit with two relaxation times and a fixed value of $r_0 = 0.315$. Such a high value of $r_0$, however, is not compatible with our results. In a later paper, Lakowicz et al. (1987) found the slightly smaller value of 3.4 ns for the long relaxation time of the tetramer, and 1.7 ns for that of the monomer. Using melittin labeled with anthraniloyl, the same group obtained three relaxation times (Maliwal et al., 1986), the longest was 14 ns for the tetramer and 3.6 ns for the monomer. Tran and Beddard (1985) detecting again the Trp fluorescence of melittin found two relaxation times, the longer one being 2.4 ns for the tetramer and 1.8 ns for the monomer. Finally, Georghiou et al. (1982), analyzing their data in terms of one relaxation time, obtained values for the monomer and tetramer close to our average relaxation times $\bar{\phi}$.

Our results for $r_0$, 0.21 and 0.24, lie at the upper end of the large range of $r_0$ values reported for Trp residues in proteins (Beecham and Brand, 1985). In this context it should be noted that our experimental resolution does permit the detection of relaxation processes down to ~50 ps, hence our relatively high $r_0$ values may be a consequence of the detection of subnanosecond relaxation processes. Under the assumption of a single pair of absorption and emission dipoles, Eq. 7 is applicable and yields for the angle between the dipoles $\phi_a - \phi_e = 31°$ and 34° for the monomer and tetramer, respectively.

## Melittin in Lipid Vesicle Membranes

The intensity and anisotropy of the Trp fluorescence of melittin incorporated into vesicle membranes of DMPC at a molar ratio of 1:150 at 36°C is shown in Fig. 2. The intensity decay is similar to the one of melittin in water, but the anisotropy decays more slowly and remains finite after 15 ns, the upper end of the time window in these measurements. The results of the fits are listed in Table II. The intensity was fitted again by a sum of three exponentials, and the lifetimes and amplitudes obtained are close to those of water-dissolved melittin. The anisotropy was fitted first by two exponentials and a residual anisotropy $r_\infty$ acording to Eq. 2. The fit was acceptable as judged by the $\chi^2$ value, the two relaxation times resulting as 1.0 and 5.6 ns with $r_\infty = 0.10$. In a fit with three relaxation times and an $r_\infty$, the value of $\chi^2$ remained essentially constant. Two fast relaxation times resulted as 0.1 and 3 ns, and a longer one as 12 ns together with $r_\infty = 0.09$. However, the error limits of the long relaxation time and of $r_\infty$ are that large that a fit with 100 ns and $r_\infty = 0$ would also be possible. This implies that the data do not permit determination of a
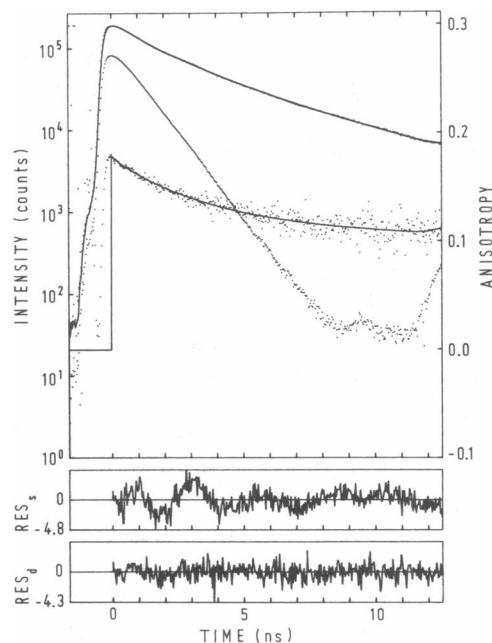


FIGURE 2  Intensity and anisotropy of the Trp fluorescence of melittin in vesicle membranes of DMPC at a molar ratio of 1:150 and 36°C. The experimental time window was 15 ns. The experimental data are shown (. . . .) together with the fits (——) and the residuals. The intensity was fitted by three exponentials and the anisotropy by three exponentials and an $r_\infty$ according to Eq. 2.

**PARAMETERS OF DIFFERENT FITS TO THE INTENSITY AND ANISOTROPY OF Trp FLUORESCENCE OF MELITTIN IN VESICLE MEMBRANES OF DMPC AT 36°C\* AND AT 19°C‡ FOR THE EXPERIMENTAL TIME WINDOW 15 ns**

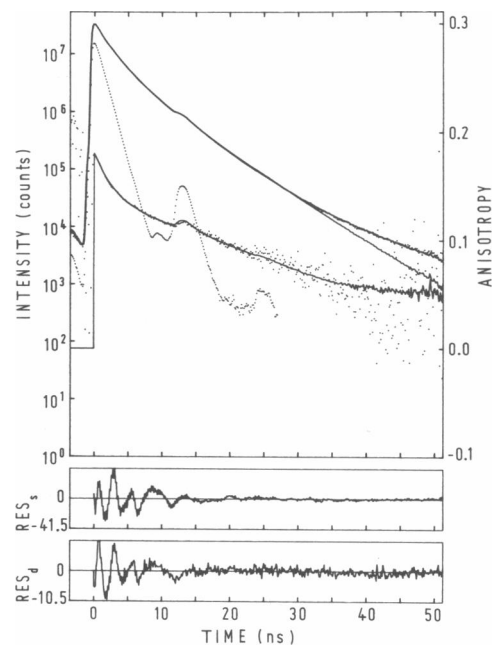| | 19°C | | 36°C | |
|---|---|---|---|---|
| $\tau_1$ (ns), $\alpha_1$ | 0.46 ± 0.01 | 0.36 ± 0.02 | 0.48 ± 0.01 | 0.36 ± 0.02 |
| $\tau_2$ (ns), $\alpha_2$ | 2.19 ± 0.08 | 0.34 ± 0.01 | 1.95 ± 0.04 | 0.41 ± 0.02 |
| $\tau_3$ (ns), $\alpha_3$ | 6.08 ± 0.09 | 0.30 ± 0.02 | 5.08 ± 0.06 | 0.32 ± 0.02 |
| $\bar{\tau}$ (ns) | 2.7 | | 2.1 | |
| $\chi^2$ | 2.49 | | 2.55 | |
| $\phi_1$ (ns), $b_1$ | 0.75 ± 0.5 | 0.018 ± 0.009 | 1.0 ± 0.6 | 0.016 ± 0.009 |
| $\phi_2$ (ns), $b_2$ | 3.3 ± 0.8 | 0.041 ± 0.009 | 5.6 ± 1.4 | 0.071 ± 0.006 |
| $r_\infty$ | | 0.114 ± 0.002 | | 0.098 ± 0.005 |
| $r_0$ | 0.173 | | 0.186 | |
| $\bar{\phi}$ (ns) | 2.5 | | 4.8 | |
| $\chi^2$ | 1.15 | | 1.10 | |
| $\phi_1$ (ns), $b_1$ | 0.12 ± 0.3 | 0.023 ± 0.08 | 0.1 ± 0.3 | 0.02 ± 0.1 |
| $\phi_2$ (ns), $b_2$ | 2.10 ± 0.6 | 0.044 ± 0.01 | 3.0 ± 4.0 | 0.05 ± 0.1 |
| $\phi_3$ (ns), $b_3$ | 43.5 ± 800 | 0.030 ± 0.04 | 12 ± 100 | 0.04 ± 0.05 |
| $r_\infty$ | | 0.091 ± 0.04 | | 0.09 ± 0.1 |
| $r_0$ | 0.189 | | 0.20 | |
| $\bar{\phi}$ (ns) | 14.4 | | 5.6 | |
| $\chi^2$ | 1.16 | | 1.12 | |

\*As shown in Fig. 2. ‡Data not shown.



FIGURE 3. Intensity and anistropy of the Trp fluorescence of melittin in vesicle membranes of DMPC at a molar ratio of 1:150 and 36°C. The experimental time window was 60 ns. The experimental data are shown (. . . .) together with the fits (———) and the residuals. The intensity was fitted by four exponentials (the fit with three exponentials is shown for comparison) and the anisotropy by two exponentials and an $r_\infty$ permitting two different emission dipoles according to Eq. 14.

relaxation time in the range of tens of nanoseconds together with a finite residual anisotropy. The reason for this failure lies in the large scatter of the data at long times or, equivalently, in the too narrow time window of 15 ns. Vogel and Rigler (1987) for the same system reported three relaxation times with a long one of 20 ns, which is not far from our result of 12 ns but subject to the same uncertainty. Our mean relaxation time $\bar{\phi}$ = 5.6 ns is comparable with the single relaxation time found by Georghiou et al. (1982) for melittin in membranes of distearoylphosphatidylcholine at 61°C.

To improve the resolution of the slow relaxation process we extended the time window to 60 ns and increased the measuring time to 24 h so that the scatter of the data at the upper end of the time window was of the same order of magnitude as previously for the smaller time window. The intensity and anisotropy obtained from such a measurement at 36°C are shown in Fig. 3 and the results of the fits are listed in Table III. It is evident from the intensity that after ~30 ns a fourth decay process begins to play a role. Its lifetime is ~10 ns with a relative amplitude <1%. The other lifetimes and amplitudes agree with those obtained for the shorter time window. A fit of the anisotropy by two exponentials and an $r_\infty$ according to Eq. 2 yielded a short relaxation time of ~2 ns and a long one of >100 ns together with $r_\infty$ = −0.21. Obviously, the two fast relaxation processes found with the shorter time window can no longer be resolved. On the other hand, the relative errors of the long relaxation time and of $r_\infty$ have decreased. The value of $r_\infty$, however, is just at the limit of its physical

range. According to Eq. 8, $r_\infty$ = −0.2 is the lowest possible value requiring $\theta_a$ = 0 and $\theta_e$ = 90°, or vice versa, and $\langle P_2 \rangle$ = 1. In that case, Eq. 7 leads to $r_0$ = −0.2, which is not compatible with the experimental result $r_0$ = 0.19. Hence, the assumption behind Eqs. 7, 8, and also 2, namely one pair of absorption and emission dipoles, is not valid here. The failure of this assumption is evident from the data of Fig. 3. In the region around 30 ns, where the additional transition with a long lifetime comes into play, the anisotropy decreases roughly linear in time. This cannot be described by a sum of exponentials as in the model with one pair of absorption and emission dipoles, but requires a more general model.

In attempting to fit the anisotropy decay by a model with two emission dipoles, we attributed the short lifetimes $\tau_1$, $\tau_2$, $\tau_3$ to one emission dipole and the long lifetime to the other. Furthermore, we assumed that there is only one absorption dipole which falls into the symmetry axis of the fluorophore. Then Eq. 14 for the anisotropy applies and a fit of this expression with two relaxation times to the anisotropy of Fig. 3 led to the parameters included in Table III. The fitted curve now remains positive at infinitely long times expressed by $r_\infty$ = 0.03. The orientational order parameter of the fluorophore results at $\langle P_2 \rangle$ = 0.55 and the angles of the two emission dipoles with respect to the symmetry axis are 36° and 44°. Most importantly, the long relaxation time is obtained as 30 ns with a small error of 3%.

## TABLE III
### PARAMETERS OF DIFFERENT FITS TO THE INTENSITY AND ANISOTROPY OF TRP FLUORESCENCE OF MELITTIN IN VESICLE MEMBRANES OF DMPC AT 36°C* AND AT 19°C‡ FOR THE EXPERIMENTAL TIME WINDOW 60 ns

| | 19°C | | 36°C | |
|---|---|---|---|---|
| $\tau_1$ (ns), $\alpha_1$ | | | $0.736 \pm 0.002$ | $0.382 \pm 0.001$ |
| $\tau_2$ (ns), $\alpha_2$ | | | $2.528 \pm 0.003$ | $0.487 \pm 0.002$ |
| $\tau_3$ (ns), $\alpha_3$ | | | $5.620 \pm 0.004$ | $0.130 \pm 0.001$ |
| $\bar{\tau}$ (ns) | | | 2.2 | |
| $\chi^2$ | | | 140.2 | |
| $\tau_1$ (ns), $\alpha_1$ | $0.455 \pm 0.004$ | $0.351 \pm 0.005$ | $0.414 \pm 0.002$ | $0.337 \pm 0.001$ |
| $\tau_2$ (ns), $\alpha_2$ | $2.28 \pm 0.02$ | $0.338 \pm 0.001$ | $1.892 \pm 0.005$ | $0.429 \pm 0.001$ |
| $\tau_3$ (ns), $\alpha_3$ | $5.41 \pm 0.04$ | $0.279 \pm 0.001$ | $4.48 \pm 0.01$ | $0.228 \pm 0.001$ |
| $\tau_4$ (ns), $\alpha_4$ | $10.3 \pm 0.1$ | $0.032 \pm 0.002$ | $10.7 \pm 0.1$ | $0.005 \pm 0.003$ |
| $\bar{\tau}$ (ns) | 2.8 | | 2.0 | |
| $\chi^2$ | 53.1 | | 54.3 | |
| $\phi_1$ (ns), $b_1$ | | | $2.41 \pm 0.03$ | $0.043 \pm 0.001$ |
| $\phi_2$ (ns), $b_2$ | | | $128 \pm 120$ | $0.35 \pm 0.06$ |
| $r_\infty$ | | | | $-.21 \pm 0.04$ |
| $r_0$ | | | | 0.187 |
| $\bar{\phi}$ (ns) | | | 114 | |
| $\chi^2$ | | | 4.90 | |
| $\phi_1$ (ns), $b_1$ | | | $2.36 \pm 0.03$ | $0.043 \pm 0.001$ |
| $\phi_2$ (ns), $b_2$ | | | $97 \pm 223$ | $0.14 \pm 0.04$ |
| $\phi_3$ (ns), $b_3$ | | | $96 \pm 240$ | $0.14 \pm 0.05$ |
| $r_\infty$ | | | | $-0.13 \pm 0.04$ |
| $r_0$ | | | | 0.187 |
| $\bar{\phi}$ (ns) | | | 84 | |
| $\chi^2$ | | | 4.93 | |
| $\phi_1$ (ns), $\beta_1$ | $1.4 \pm 0.1$ | 0.110 | $2.4 \pm 0.1$ | 0.089 |
| $\phi_2$ (ns), $\beta_2$ | $27.1 \pm 2.6$ | $0.11 \pm 0.04$ | $30.4 \pm 1.1$ | $0.19 \pm 0.02$ |
| $\langle P_2 \rangle$, $\beta_3$ | 0.67 | $0.181 \pm 0.002$ | 0.55 | $0.12 \pm 0.05$ |
| $P_2 (\theta_{e1})$, $\theta_{e1}$ | $0.45 \pm 0.02$ | 37° | $0.47 \pm 0.07$ | 36° |
| $P_2 (\theta_{e2})$, $\theta_{e2}$ | $0.3 \pm 0.1$ | 42° | $0.26 \pm 0.10$ | 44° |
| $r_\infty$ | | 0.058 | | 0.031 |
| $r_0$ | | 0.162 | | 0.187 |
| $\bar{\phi}$ (ns) | 14.1 | | 21.4 | |
| $\chi^2$ | 3.40 | | 4.96 | |

*As shown in Fig. 3. ‡Data not shown.

In the ordered lipid phase at 19°C, such an analysis yields the same values for the angles of the emission dipoles and also approximately the same value for the long relaxation time. Only the order parameter increases to $\langle P_2 \rangle = 0.67$.

## Melittin in a Dry Lipid Film

Under conditions where the fluorophore is completely immobilized the anisotropy should remain constant in time for the case of one transition or, for the case of two transitions, should vary according to the varying contributions of the two transitions to the intensity. Therefore, we investigated melittin in a dry film consisting of an equimolar mixture of melittin and DMPC. The intensity and anisotropy of the Trp fluorescence for a time window of 60 ns are shown in Fig. 4 and the results of the fits listed in Table IV. A fit of the anisotropy by Eq. 2 for one pair of absorption and emission dipoles and two relaxation times
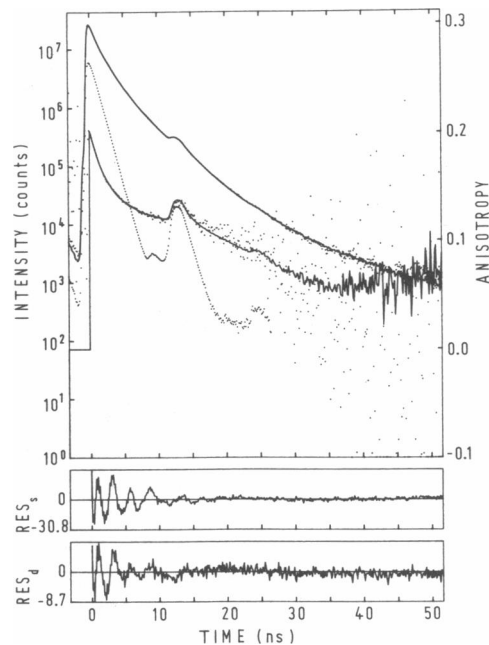


FIGURE 4 Intensity and anisotropy of the Trp fluorescence of melittin in a film of DMPC at a molar ratio of 1:1 and 19°C. Other conditions as in Fig. 3.

yields the value $r_\infty = -0.9$ which is far outside its physically possible range. If the anisotropy is fitted by Eq. 14 for two emission dipoles and two relaxation times, $r_\infty$ remains positive and the orientational order parameter results as 0.76. This value is slightly higher than the order parameter in the ordered lipid phase, but still smaller than

## TABLE IV
### PARAMETERS OF DIFFERENT FITS TO THE INTENSITY AND ANISOTROPY OF Trp FLUORESCENCE OF MELITTIN IN A FILM OF DMPC FOR TIME WINDOWS OF 60 ns* AND 15 ns‡

| | 15 ns | | 60 ns | |
|---|---|---|---|---|
| $\tau_1$ (ns), $\alpha_1$ | $0.44 \pm 0.02$ | $0.292 \pm 0.010$ | $0.473 \pm 0.003$ | $0.463 \pm 0.001$ |
| $\tau_2$ (ns), $\alpha_2$ | $2.03 \pm 0.06$ | $0.440 \pm 0.005$ | $1.63 \pm 0.007$ | $0.395 \pm 0.002$ |
| $\tau_3$ (ns), $\alpha_3$ | $4.49 \pm 0.08$ | $0.268 \pm 0.015$ | $3.70 \pm 0.014$ | $0.398 \pm 0.001$ |
| $\tau_4$ (ns), $\alpha_4$ | — | | $10.2 \pm 0.2$ | $0.0021 \pm 0.0002$ |
| $\bar{\tau}$ (ns) | 2.2 | | 1.4 | |
| $\chi^2$ | 2.07 | | 31.0 | |
| $\phi_1$ (ns), $b_1$ | $1.1 \pm 0.8$ | $0.025 \pm 0.025$ | $1.95 \pm 0.02$ | $0.067 \pm 0.004$ |
| $\phi_2$ (ns), $b_2$ | $3.7 \pm 1.3$ | $0.069 \pm 0.025$ | $406 \pm 15$ | $1.05 \pm 0.04$ |
| $r_\infty$ | | $0.103 \pm 0.003$ | | $-0.90 \pm 0.03$ |
| $r_0$ | | 0.198 | | 0.213 |
| $\bar{\phi}$ (ns) | 3.0 | | 382 | |
| $\chi^2$ | 1.02 | | 3.37 | |
| $\phi_1$ (ns), $\beta_1$ | | | $1.7 \pm 1.1$ | 0.087 |
| $\phi_2$ (ns), $\beta_2$ | | | $4.72 \pm 0.07$ | $0.084 \pm 0.004$ |
| $\langle P_2 \rangle$, $\beta_3$ | | | 0.76 | $0.230 \pm 0.035$ |
| $P_2 (\theta_{e1})$, $\theta_{e1}$ | | | $0.53 \pm 0.09$ | 34° |
| $P_2 (\theta_{e2})$, $\theta_{e2}$ | | | $0.15 \pm 0.1$ | 49° |
| $r_0$ | | | | 0.213 |
| $\bar{\phi}$ (ns) | | | 3.2 | |
| $\chi^2$ | | | 3.25 | |

*As shown in Fig. 4. ‡Data not shown.

one. Hence, the fluorophore is not completely immobilized. The slow relaxation process with 30 ns, however, is absent. The two relaxation times obtained are both relatively small and similar to those found with melittin in vesicle membranes for the small time window. Most relevant in our context is the result that the angles of the emission dipoles of the two transitions with respect to the symmetry axis agree fairly well with their values obtained above for melittin in vesicle membranes.

### Melittin Labeled with Pyrene-Maleimide in Lipid Vesicle Membranes

The difficulties arising from the short lifetime of the Trp fluorescence in determining long relaxation times may be circumvented by using a fluorescence label with a longer lifetime. For that reason, we labeled melittin with MalNPyr, which is known to have a lifetime component of $\sim$100 ns (Weltman et al., 1973). The fluorescence intensity and anisotropy of MalNPyr-melittin in vesicle membranes of DMPC at a molar ratio of 1:200 and 36°C are shown in Fig. 5. The intensity decays so slowly that even for a time window of 180 ns not more than 1 h measuring time is required. The anisotropy shows a relaxation process with a characteristic time in the range of 20–30 ns and at large times levels off of a finite value. The results of the fits are listed in Table V. The intensity decays with three lifetimes, one of them being $\sim$100 ns as expected. The anisotropy could be fitted reasonably well by two exponentials and a residual anisotropy $r_\infty$, but the goodness of the fit improved

**TABLE V**

PARAMETERS OF DIFFERENT FITS OF THE INTENSITY AND ANISOTROPY OF THE FLUORESCENCE OF MalNPyr-MELITTIN IN VESICLE MEMBRANES OF DMPC AT 36°C* AND AT 17°C‡

| | 17°C | | 36°C | |
|---|---|---|---|---|
| $\tau_1$ (ns), $\alpha_1$ | 8.8 ± 0.5 | 0.36 ± 0.05 | 9.23 ± 0.15 | 0.61 ± 0.03 |
| $\tau_2$ (ns), $\alpha_2$ | 16.4 ± 0.6 | 0.48 ± 0.05 | 17.8 ± 0.6 | 0.26 ± 0.03 |
| $\tau_3$ (ns), $\alpha_3$ | 135.7 ± 1.0 | 0.162 ± 0.001 | 93.4 ± 0.5 | 0.134 ± 0.001 |
| $\bar{\tau}$ (ns) | 33.0 | | 22.7 | |
| $\chi^2$ | 4.61 | | 9.48 | |
| | | | | |
| $\phi_1$ (ns), $b_1$ | 1.0 ± 0.2 | 0.06 ± 0.02 | 3.9 ± 0.2 | 0.086 ± 0.003 |
| $\phi_2$ (ns), $b_2$ | 32 ± 1 | 0.088 ± 0.001 | 21.6 ± 0.9 | 0.090 ± 0.003 |
| $r_\infty$ | | 0.099 ± 0.001 | | 0.029 ± 0.001 |
| $r_0$ | | 0.247 | | 0.206 |
| $\bar{\phi}$ (ns) | 19.7 | | 13.0 | |
| $\chi^2$ | 1.26 | | 1.21 | |
| | | | | |
| $\phi_1$ (ns), $b_1$ | 0.7 ± 0.2 | 0.08 ± 0.05 | 2.2 ± 0.5 | 0.05 ± 0.01 |
| $\phi_2$ (ns), $b_2$ | 19 ± 7 | 0.06 ± 0.03 | 9.6 ± 2.0 | 0.09 ± 0.01 |
| $\phi_3$ (ns), $b_3$ | 75 ± 60 | 0.05 ± 0.02 | 37.5 ± 10 | 0.05 ± 0.01 |
| $r_\infty$ | | 0.09 ± 0.01 | | 0.026 ± 0.001 |
| $r_0$ | | 0.277 | | 0.210 |
| $\bar{\phi}$ (ns) | 24.2 | | 14.5 | |
| $\chi^2$ | 1.23 | | 1.15 | |

*As shown in Fig. 5. ‡Data not shown.

upon inclusion of a third relaxation process. The long relaxation time results as 37.5 ns which, within the error limits, agrees with the long relaxation time of the Trp anisotropy. The two short relaxation times are $\sim$2 and 10 ns. Similar results were obtained by Maliwal et al. (1986) using melittin with an anthraniloyl label. The longest of their three relaxation times found was 47 ns which is close to our value. If Eqs. 9 and 10 are used to determine the orientational order parameters of the MalNPyr label, one obtains for the total order parameter $\langle P_2 \rangle = 0.35$ and for the order parameter of the slow fluctuations $\langle P_2 \rangle_s = 0.61$, so that the order parameter for the fast fluctuations becomes $\langle P_2 \rangle_f = 0.57$.

Although the MalNPyr anisotropy could well be fitted under the assumption of one pair of absorption and emission dipoles, fits involving two emission dipoles were also performed. As expected, they did not lead to an improvement indicating that the emission dipoles of the short and long lifetime components coincide.

In the ordered lipid phase at 17°C, the fit with two relaxation times is more reliable than the one with three relaxation times. The long relaxation time results as 32 ns which is close to that obtained in the fluid phase at 36°C. The total order parameter is $\langle P_2 \rangle = 0.63$ and the slow order parameter $\langle P_2 \rangle_s = 0.73$ so that $\langle P_2 \rangle_f = 0.86$.

### Pyrene-Maleimide in Lipid Vesicle Membranes

Attempting to assign the relaxation processes observed with MalNPyr-melittin to distinct fluctuations it would be
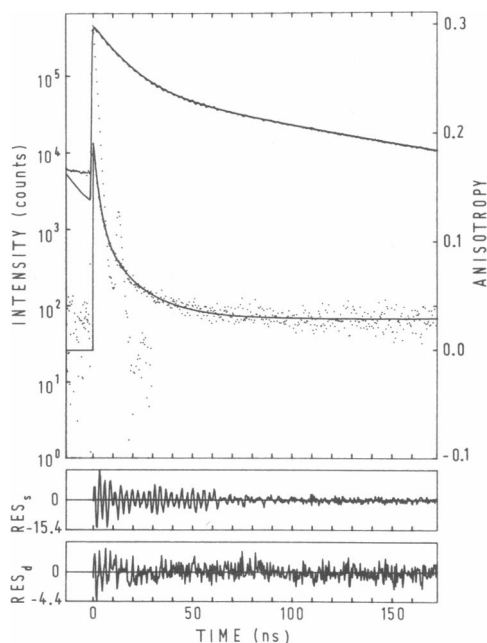


FIGURE 5 Intensity and anisotropy of the fluorescence of MalNPyr-melittin in vesicle membranes of DMPC at a molar ratio of 1:200 and 36°C. The experimental data are shown (. . . .) together with the fits (——) and the residuals. The intensity was fitted by three exponentials and the anisotropy by three exponentials and an $r_\infty$ according to Eq. 2.

useful to know how the MalNPyr fluorophore alone fluctuates in a lipid membrane. Therefore, we performed FAD measurements on a MalNPyr derivative which closely resembles the MalNPyr label attached to melittin, namely the product of the reaction of MalNPyr with mercaptoethanol, MalNPyr-MEt. The intensity and anisotropy of MalNPyr-MEt in vesicle membranes of DMPC at 36°C are shown in Fig. 6 and the results of the fits are listed in Table VI. The intensity could be fitted by three exponentials as in the case of MalNPyr-melittin, but the individual lifetimes and amplitudes are somewhat different and lead to a much larger average lifetime of 80 ns. The anisotropy could well be fitted by two exponentials and a residual anisotropy $r_\infty$. The two relaxation times result as 2 and 8 ns, which implies the absence of the slow relaxation process observed with MalNPyr-melittin. Calculation of the order parameter of the fluorophore according to Eq. 9 yields $\langle P_2 \rangle = 0.19$, a much smaller value than obtained for MalNPyr-melittin.

In the ordered lipid phase at 17°C, the two relaxation times are considerably longer. Also the residual anisotropy has increased leading to an order parameter $\langle P_2 \rangle = 0.45$.

## DISCUSSION

### Melittin in Water

The aim in interpreting FAD data is to assign the observed relaxation processes to different kinds of orientational fluctuations of the fluorophore. If the fluorophore is part of a polypeptide as in our case, it may undergo fluctuations relative to the backbone and, in addition, may reflect
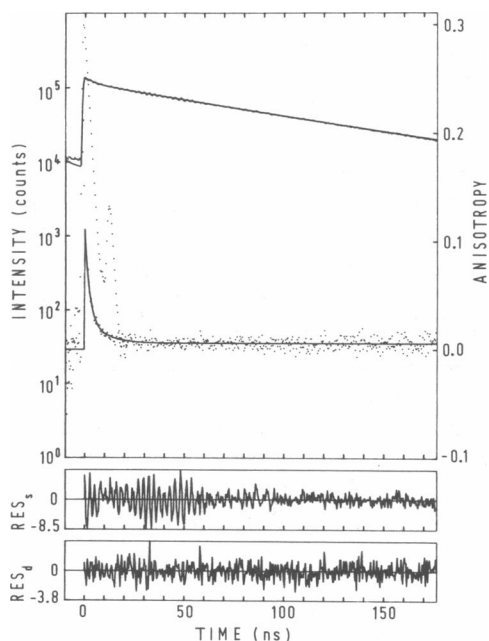


FIGURE 6   Intensity and anisotropy of the fluorescence of MalNPyr-MEt in vesicle membranes of DMPC at a molar ratio of 1:200 and 36°C. Other conditions as in Fig. 5.

TABLE VI
PARAMETERS OF DIFFERENT FITS TO THE INTENSITY AND ANISOTROPY OF THE FLUORESCENCE OF MalNPyr-MEt IN VESICLE MEMBRANES OF DMPC AT 36°C* AND AT 19°C‡

| | 17°C | | 36°C | |
|---|---|---|---|---|
| $\tau_1$ (ns), $\alpha_1$ | 3.2 ± 0.4 | 0.13 ± 0.01 | 4.85 ± 0.15 | 0.199 ± 0.005 |
| $\tau_2$ (ns), $\alpha_2$ | 15.3 ± 0.5 | 0.129 ± 0.001 | 51 ± 9 | 0.14 ± 0.05 |
| $\tau_3$ (ns), $\alpha_3$ | 156 ± 1 | 0.74 ± 0.01 | 108 ± 3 | 0.67 ± 0.05 |
| $\bar{\tau}$ (ns) | 118 | | 80 | |
| $\chi^3$ | 4.92 | | 6.19 | |
| | | | | |
| $\phi_1$ (ns), $b_1$ | 7.3 ± 1.1 | 0.048 ± 0.004 | 2.2 ± 0.3 | 0.13 ± 0.01 |
| $\phi_2$ (ns), $b_2$ | 44 ± 3 | 0.075 ± 0.004 | 8.3 ± 1.7 | 0.03 ± 0.01 |
| $r_\infty$ | | 0.031 ± 0.001 | | 0.006 ± 0.001 |
| $r_0$ | | 0.155 | | 0.172 |
| $\bar{\phi}$ (ns) | 29.9 | | 3.4 | |
| $\chi^3$ | 1.25 | | 1.09 | |

*As shown in Fig. 6. ‡Data not shown.

fluctuations of the backbone up to rotational diffusion of the entire polypeptide or an aggregate of polypeptides.

For melittin dissolved in water as a tetramer we found three relaxation processes with 0.16, 1.2, and 5.6 ns. The size and shape of the tetramer is rather well known because it is essentially the same tetramer as in the crystal structure of melittin (Terwilliger et al., 1982). Hence, the relaxation time for rotational diffusion of it can be estimated theoretically. In good approximation, the tetramer can be described as a sphere, so that according to Perrin (1936),

$$\phi_r = \frac{1}{6D_r}, \tag{15}$$

with the coefficient for rotational diffusion given by

$$D_r = \frac{kT}{6\eta V}. \tag{16}$$

The volume of the tetramer is $V = 1.4 \cdot 10^{-20}$ cm$^3$, based on a mol wt of 2,858 for the melittin monomer and a density of 1.4 g/cm$^3$ (Terwilliger et al., 1982). The viscosity of water at 20°C and 2M NaCl is $\eta = 1.24$ cp. Hence, one obtains $D_r = 4 \cdot 10^7$ s$^{-1}$ and $\phi_r = 4.2$ ns. This value is close to the long relaxation time of 5.5 ns found experimentally, so that we assign this slow relaxation process to rotational diffusion of the tetramer. The small difference between calculated and measured rotational relaxation times has been attributed in other cases to the hydration shell of proteins (Beecham and Brand, 1985).

The above assignment of the slow relaxation process to rotational diffusion is also compatible with the result for the monomer. Its slow relaxation time is found by a factor of four smaller than that of the tetramer. This would be expected according to Eqs. 15 and 16, if the monomer also has a spherical shape. Such a conclusion, however, must not necessarily be drawn, the observed slow relaxation

process of the monomer could as well reflect a segmental motion of the unfolded polypeptide chain.

The fast relaxation process in the 100 ps range observed for monomeric and tetrameric melittin may correspond to fluctuations of the Trp side chain relative to the polypeptide backbone. Such an assignment is supported by molecular dynamics simulations (Ichiye and Karplus, 1983). For tetrameric melittin a further process with a relaxation time of 1 ns is observed, which may reflect fluctuations of the four helices against each other or of two segments of one helix against each other.

## Melittin in Membranes

The viscosity of a lipid membrane is three orders of magnitude higher than that of water (Peters and Cherry, 1982). Hence, the rotational diffusion of melittin in membranes, either aggregated or not, is of the order of a microsecond and thus undetectable in our experiments. Fluctuations of restricted amplitude of the melittin helix and fluctuations of the fluorophores relative to the helix backbone remain possible candidates for the assignment of the observed relaxation processes.

Two fast relaxation processes with 0.1 and 3 ns were found in the Trp anisotropy and, similarly, two fast relaxation processes with 2 and 10 ns in the MalNPyr anisotropy of melittin. The MalNPyr label alone dissolved as MalNPyr-MEt in a lipid membrane showed approximately the same two relaxation times, suggesting that the two fast relaxation processes of the MalNPyr label attached to melittin correspond to fluctuations of that label relative to the backbone. One is tempted to assign, by analogy, the two fast Trp relaxation processes to fluctuations of the Trp side chain. For the subnanosecond relaxation process this is consistent with the assignment in the case of water-dissolved melittin, for the 3 ns relaxation process this assignment remains speculative.

In addition to the two fast relaxation processes, the Trp as well as the MalNPyr anisotropy of melittin in membranes exhibits a slow process with a relaxation time of 35 ns. The coincidence of the two relaxation times points to a common origin of the relaxation processes and we, therefore, assign them to fluctuations of the polypeptide backbone which is the same for Trp and MalNPyr, namely a helix. The relaxation time of helix fluctuations may be estimated theoretically by describing the helix as a symmetric ellipsoid which undergoes orientational fluctuations in an ordering potential (van der Meer et al., 1984). In the limit of high order one obtains (Dornmair, K., and F. Jähnig, submitted for publication).

$$\phi = \frac{\langle \vartheta^2 \rangle}{2D_\perp}.$$ (17)

Here, $\langle \vartheta_2 \rangle$ denotes the mean-square fluctuations of the angle $\vartheta$ specifying the instantaneous orientation of the long axis relative to its mean orientation, and $D_\perp$ represents the

coefficient for rotational diffusion about a short axis. $D_\perp$ can be calculated from the relation (Perrin, 1936; Memming, 1961)

$$D_\perp = \frac{3kT}{16\pi\eta a^3}\left(2 \ln \frac{2a}{b} - 1\right),$$ (18)

with $a$ and $b$ denoting the half axes of the ellipsoid. Using $2a = 30$ Å and $2b = 10$ Å to simulate the melittin helix and 1 p for the viscosity of a lipid membrane, one obtains $D_\perp = 2 \cdot 10^6 \, \text{s}^{-1}$. The mean-square fluctuations $\langle \vartheta^2 \rangle$ can be determined from experiment. The slow order parameter is defined as $\langle P_2 \rangle_s = \langle (3 \cos^2\vartheta - 1)/2 \rangle$, which in the limit of high order becomes $\langle P_2 \rangle_s = 1 - 3/2 \langle \vartheta^2 \rangle$. The experimental value $\langle P_2 \rangle_s = 0.61$, obtained from the MalNPyr anisotropy, yields $\langle \vartheta^2 \rangle = 0.26$. Insertion into Eq. 17 leads to $\phi = 65$ ns. This value is a rough estimate, but its order of magnitude supports the notion that the slow relaxation process observed with Trp and MalNPyr corresponds to orientational fluctuations of the melittin helix.

In this assignment, the melittin helices fluctuate about axes which remain unspecified. If one adopts the model of Vogel and Jähnig (1986) in which melittin forms a bundle of four membrane-spanning helices, the helix fluctuations become fluctuations of membrane-spanning helices. The helices undergo a wobbling motion about the membrane normal.

A slow relaxation process with a relaxation time of ~40 ns has been detected in FAD measurements on lactose permease of *Escherichia coli*, a membrane protein which transports galactosides across the cytoplasmic membrane (Dornmair, K., and F. Jähnig, submitted for publication). There is good evidence that this protein is folded into 10–14 membrane-spanning helices (Vogel et al., 1985). Therefore, also in that case the slow relaxation process was assigned to fluctuations of membrane-spanning helices. A correlation between helix fluctuations and the transport function could even be demonstrated—under conditions where transport is reduced, the helix fluctuations are also slowed down and decreased in amplitude. Whether such a correlation also exists for melittin remains to be investigated. Helix fluctuations might, for example, be necessary as a trigger for the opening of the melittin pore upon imposition of a membrane potential.

As a final remark, it should be mentioned that during this FAD study on melittin some new insight into the fluorescence of Trp and MalNPyr was gained. Control measurements on NATA were also performed. A full discussion of this topic, however, is beyond the scope of this paper and will be presented elsewhere.

## REFERENCES

Beecham, J. M., and L. Brand. 1985. Time-resolved fluorescence of proteins. *Annu. Rev. Biochem.* 54:43–71.

Berlman, I. 1971. Handbook of Fluorescence Spectra of Aromatic Molecules. Academic Press, New York. 298.

Best, L., E. John, and F. Jähnig. 1987. Order and fluidity of lipid membranes as determined by fluorescence anistropy decay. *Eur. Biophys. J.* 15:87–102.

Dufourc, E. J., J. F. Faucon, G. Fourche, J. Dufourcq, T. Gulik-Krzywicki, and M. le Maire. 1986. Reversible disc-to-vesicle transition of melittin-DPPC complexes triggered by the phospholipid acyl chain melting. *FEBS (Fed. Eur. Biochem. Soc.) Lett.* 201:205–209.

Georghiou, S., M. Thompson, and A. K. Mukhopadhyay. 1982. Melittin-phospholipid interaction studied by employing the single trytophan residue as an intrinsic fluorescent probe. *Biochim. Biophys. Acta.* 688:441–452.

Hanke, W., C. Methfessel, H. U. Wilmsen, E. Katz, G. Jung, and G. Boheim. 1983. Melittin and a chemically modified trichotoxin form alamethicin-type multi-state pores. *Biochim. Biophys. Acta.* 727:108–114.

Hermetter, A., and J. R. Lakowicz. 1986. The aggregation state of melittin in lipid bilayers. *J. Biol. Chem.* 26:8243–8248.

Ichiye, T., and M. Karplus. 1983. Fluorescence depolarization of trytophan residues in proteins: a molecular dynamics study. *Biochemistry.* 22:2884–2893.

Jähnig, F. 1979. Structural order of lipids and proteins in membranes: evaluation of fluorescence anistropy data. *Proc. Natl. Acad. Sci. USA.* 76:6361–6365.

Kempf, C., R. D. Klausner, J. N. Weinstein, J. Van Renswonde, M. R. Pincus, and R. Blumenthal. 1982. Voltage-dependent trans-bilayer orientation of melittin. *J. Biol. Chem.* 257:2469–2476.

Lakowicz, J. R., G. Laczko, I. Gryczynski, and H. Cherek. 1986. Measurement of subnanosecond anistropy decay of protein fluorescence using frequency-domain fluorometry. *J. Biol. Chem.* 261:2240–2245.

Lakowicz, J. R., H. Cherek, I. Grycyznski, N. Joshi, and M. L. Johnson. 1987. Enhanced resolution of fluorescence anistropy decays by simultaneous analysis of progressively quenched samples. *Biophys. J.* 51:755–768.

Lambert, R. A., L. A. Chewter, D. Phillips, D. V. O'Connor, A. J. Roberts, and S. R. Meech. 1983. Standards for nanosecond fluorescence decay time measurements. *Anal. Chem.* 55:68–73.

Lavialle, F., R. G. Adams, and I. W. Levin. 1982. Infrared spectroscopic study of the secondary structure of melittin in water, 2-chloroethanol, and phospholipid bilayer dispersions. *Biochemistry.* 21:2305–2312.

Maliwal, B. P., A. Hermetter, and J. R. Lakowicz. 1986. A study of protein dynamics from anistropy decay obtained by variable frequency phase-modulation fluorometry: internal motions of N-methylanthraniloyl melittin. *Biochim. Biophys. Acta.* 873:173–181.

Memming, R. 1961. Theorie der Fluoreszenzpolarisation für nicht kugelsymmetrische Moleküle. *Z. Phys. Chem.* 28:168–189.

Perrin, F. 1936. Mouvement brownien d'un ellipsoide. II. Rotation libre et dépolarisation des fluorescences. Translation et diffusion des molécules ellipsoidales. *J. Phys. Radium.* 7:1–11.

Peters, R., and R. J. Cherry. 1982. Lateral and rotational diffusion of bacteriorhodopsin in lipid bilayers: experimental test of the Saffman-Delbrück equations. *Proc. Natl. Acad. Sci. USA.* 79:4317–4321.

Quay, S. C., and C. C. Condie. 1983. Conformational studies of aqueous melittin: thermodynamic parameters of the monomer-tetramer self-association reaction. *Biochemistry.* 22:695–700.

Stanislawski, B., and H. Rüterjans. 1987. $^{13}$C-NMR investigation of the insertion of the bee venom melittin into lecithin vesicles. *Eur. Biophys. J.* 15:1–12.

Szabo, A. 1980. Theory of polarized fluorescent emission in uniaxial liquid crystals. *J. Chem. Phys.* 72:4620–4626.

Talbot, J. C., J. Dufourcq. J. de Bony, J. F. Faucon, and C. Lussan. 1979. Conformational change and self-association of monomeric melittin. *FEBS (Fed. Eur. Biochem. Soc.) Lett.* 102:191–193.

Talbot, J. C., J. F. Faucon, and J. Dufourcq. 1987. Different states of self-association of melittin in phospholipid bilayers. *Eur. Biophys. J.* 15:147–157.

Terwilliger, T. C., L. Weissman, and D. Eisenberg. 1982. The structure of melittin in the form I crystals and its implication for melittin's lytic and surface activities. *Biophys. J.* 37:353–361.

Tosteson, M. T., and D. C. Tosteson. 1981. The sting. Melittin forms channels in lipid bilayers. *Biophys. J.* 36:109–116.

Tosteson, M. T., J. J. Levy, L. H. Caporale, M. Rosenblatt, and D. C. Tosteson. 1987. Solid-phase synthesis of melittin-purification and functional characterization. *Biochemistry.* 26:6627–6631.

Tran, C. D., and G. S. Beddard. 1985. Studies of the fluorescence from tryptophan in melittin. *Eur. Biophys. J.* 13:59–64.

Turko, B. T., J. A. Nairn, and K. Sauer. 1983. Single-photon timing system for picosecond fluorescence lifetime measurements. *Rev. Sci. Instrum.* 54:118–120.

van der Meer, W., H. Pottel, W. Herreman, M. Ameloot, H. Hendricks, and H. Schröder. 1984. Effect of orientational order on the decay of the fluorescence anisotropy in membrane suspensions. A new approximate solution of the rotational diffusion equation. *Biophys. J.* 46:515–523.

Vogel, H. 1987. Comparison of the conformation and orientation of alamethicin and melittin in lipid membranes. *Biochemistry.* 26:4562–4572.

Vogel, H., and F. Jähnig. 1986. The structure of melittin in membranes. *Biophys. J.* 50:573–582.

Vogel, H., and R. Rigler. 1987. Orientational fluctuations of melittin in lipid membranes as detected by time-resolved fluorescence anisotropy measurements. *In* Structure, Dynamics and Function of Biomolecules. A. Ehrenberg, R. Rigler, A. Gräslund, and L. Nilsson, editors. Springer-Verlag, Berlin. 289–294.

Vogel, H., F. Jähnig, V. Hoffmann, and J. Stümpel. 1983. The orientation of melittin in lipid membranes. A polarized infrared spectroscopic study. *Biochim. Biophys. Acta.* 733:201–209.

Vogel, H., J. K. Wright, and F. Jähnig. 1985. The structure of the lactose permease derived from Raman spectroscopy and prediction methods. *EMBO (Eur. Mol. Biol. Org.) J.* 4:3625–3631.

Weltman, J. K., R. P. Szaro, A. R. Frankelton, R. M. Dowben, J. R. Bunting, and R. E. Cathou. 1973. N-(3-Pyrene)maleimide: A long lifetime fluorescent sulfhydryl reagent. *J. Biol. Chem.* 248:3173–3177.

Wijnaendts van Resandt, R. W., R. H. Vogel, and S. W. Provencher. 1982. Double-beam fluorescence lifetime spectrometer with subnanosecond resolution: application to aqueous tryptophan. *Rev. Sci. Instrum.* 53:1392–1397.

Zannoni, C. 1981. A theory of fluorescence depolarization in membranes. *Mol. Phys.* 42:1303–1320.